



## The cooling efficiency of variable greenery coverage ratios in different urban densities: A study in a subtropical climate



Wanlu Ouyang <sup>a,\*</sup>, Tobi Eniolu Morakinyo <sup>b,e</sup>, Chao Ren <sup>b,c</sup>, Edward Ng <sup>a,b,d</sup>

<sup>a</sup> School of Architecture, The Chinese University of Hong Kong, New Territories, Hong Kong, China

<sup>b</sup> Institute of Future Cities, The Chinese University of Hong Kong, New Territories, Hong Kong, China

<sup>c</sup> Faculty of Architecture, The University of Hong Kong, Hong Kong, China

<sup>d</sup> Institute of Environment, Energy and Sustainability, The Chinese University of Hong Kong, New Territories, Hong Kong, China

<sup>e</sup> School of Geography, University College Dublin, Dublin 4, Ireland

### ARTICLE INFO

#### Keywords:

Urban heat island  
Urban greenery  
Cooling efficiency  
Urban density  
ENVI-met  
Urban planning

### ABSTRACT

Urban greenery, especially trees, has been proven to be one of the effective measures for urban heat island mitigation. However, no consistent findings have been found for the relationship between greenery abundance and cooling magnitude; while some previous studies discovered a linear relationship, others opined it could a non-linear one. In addition, there are rare studies exploring whether or not the strength of the relationship is dependent on urban density. Therefore, in this study, we aim to discuss cooling efficiency by measuring the relationship between greenery coverage ratio and the cooling effects of greenery. Parametric studies were conducted in a validated ENVI-met model, with different combinations of urban densities (Low, Mid, and High) and tree coverage ratios (2–30% at 2% interval, and 56% for full area coverage other than building). Then the pattern of the cooling efficiency was explored under three urban densities scenarios and two selected temporal periods on a typical summer daytime. For a subtropical climate background, results showed a non-linear (logarithmic) pattern for tree coverage ratio (TCR) and cooling effects, irrespective of the urban density, temporal periods, and heat indicators. When TCR reached 20–30%, the optimal cooling efficiency of trees were achieved, irrespective of building densities and temporal periods. The optimal threshold for greenery coverage in this study can provide science-based suggestions to urban planners and designers for better microclimate and thermal comfort environments at the neighborhood scale.

## 1. Introduction

### 1.1. Background

Due to rapid urbanization, pervious surfaces including soil and natural landscapes, have been extensively replaced by concrete and other impervious man-made materials. All of these environmental changes lead to the alteration of urban energy balance and consequently the formation of the urban heat island phenomenon (UHI) in cities. Such rapid urbanization is expected to continue especially in (sub) tropical climate regions by 2030–2050 [1], which may host more merging mega cities and large population of new immigrants. UHI effect can be intensified given the global warming and enlarging urban density, which may bring multiple negative impacts, such as expanded economic costs [2], increased extra cooling energy consumption [3,4], worsened

air quality [5], and impaired public health [6]. Especially for outdoor thermal environment, heat stress seems to be more frequently along with all these changes, which will influence citizens' health conditions and even cause health risks [7].

There has been a worldwide vision and call from United Nations to achieve sustainable development goals for cities [8]. Among the proposed climate change mitigation and adaptation strategies [9], urban greenery has been regarded as the most popular, suitable and efficient one for climate regulation. In terms of urban cooling, some studies have suggested the magnitude of cooling was directly proportional to the greenery coverage [10,11]. However, this conclusion is far from being holistic, since the cooling effects vary significantly based on different contexts [12,13]. Particularly, little is known about the optimum types, coverage ratio, and distribution of urban greenery, although these factors are necessary for optimal heat mitigation strategies at neighborhood

\* Corresponding author.

E-mail address: [wanlu.oy@link.cuhk.edu.hk](mailto:wanlu.oy@link.cuhk.edu.hk) (W. Ouyang).

and street canyon scales [14]. Therefore, this study tries to make efforts towards optimal greenery abundance for the thermal environment.

### 1.2. Relationship between greenery coverage ratio and cooling effects

In the literature, conflicting conclusions exist on the relationship between greenery coverage ratio (GCR) and the cooling effects. While some indicated linear relationship, others revealed non-linear patterns, which is due to the differences in applied methodology-whether modeling or measurement, and different urban canopy layers-land surface temperature, ambient air temperature, and surface energy fluxes.

Land surface temperature, derived from satellite images by using remote sensing technology, was found to non-linearly related to greenery coverage in some studies [15–17], and linearly dependent on greenery abundance measured by coverage ratio [15]. This difference may come from different satellite image resources and land surface characteristics in different study areas. Even within the same study, both linear and non-linear patterns have been revealed between LST and vegetation fraction [15]; the difference came from vegetation types (i.e., grass and tree) and analytical periods (i.e., diurnal and nocturnal).

In terms of near-surface air temperature, both linear [18–22] and non-linear relationships [23–25] were found by either field measurement or numerical simulation modeling. The discrepancies could be ascribed to different sampling or location density in survey points, modeling intervals for greenery coverages, as well as inconsistent indices for greenery and cooling effects. For instance, in a monitoring study, both regression patterns were found for different parameters measuring greenery: air temperature was found to increase linearly with expanding cooling distance and increasing non-linearly with higher greenery coverage [23]. In a modeling study, different patterns were found for different heat indicators: linear for AT and non-linear for physiological equivalent temperature (PET) based on the regression analysis [26].

As for Surface energy fluxes, the non-linear relationship between latent heat fluxes proportion (e.g., Bowen ratio) and the vegetative fraction was discovered in numerical simulations [27,28]. With a 3D geometry physical model, a linear pattern was detected between evaporation heat loss and the vegetative cover [29]. This difference not only relied on different modeling methods (numerical vs. physical modeling) but also arose from different quantifications for vegetation fraction: the former was the horizontal surface fraction while the latter considered whole surfaces of buildings in three-dimensional spaces.

### 1.3. Greenery cooling intensity, cooling efficiency and threshold

For linear relationships, empirical models are developed for estimating the cooling benefit per unit increase in greenery (i.e., per percent in tree coverage ratio). For instance, through field measurement, previous studies found with every 10% increase in greenery coverage, the ambient temperature in the afternoon (14:00–15:00) decreased by 0.12 °C in Beijing, China [20], and by 0.43 °C in Nagoya, Japan [19]. With numerical simulations, ambient temperature at 15:00 was estimated to decrease 0.22 °C for Beijing, China, and 1.4 °C for Arizona, USA per 10% increase in tree coverage [21,30]. Also, surface temperature was cooled by 2.71 °C in daytime and 5.74 °C in nighttime during summer for 20% increase in tree coverage in Phoenix, USA [15], while in Manchester, UK, surface temperature reduction was 2 °C for every 10% increase in tree and shrub coverage during 9:00–21:00 [31]. However, these cooling intensity per greenery coverage is not necessarily comparable due to complex interactions in urban climate studies, including different climate backgrounds, various built environment contexts, different temporal periods for analysis, and even selections in research methods.

The non-linear pattern, not changing at steady rate as the linear trend, can imply the range of the cooling benefits. The threshold for greenery coverage has significant implications for urban greenery planning and climatic-sensitive design. For instance, in Madison, USA,

tree canopy coverage was recommended to be 40% to provide the optimal increase in cooling benefits [24]. In Phoenix, USA, 40% in grass coverage and 30% in tree coverage were suggested to effectively reduce the land surface temperature [15]. Another study concluded 20–30% of vegetation fraction provided the highest proportion of latent heat flux in some North American cities [28,29]. Likewise, cooling efficiency is another focus for some greenery studies, whose target is to achieve higher potential cooling effects with less land or water consumptions as possible. Generally, the cooling efficiency refers to the ratio between cooling intensity and the consumed resources (i.e., land, water, etc.), although it is defined differently according to different measurement index and research objectives [1,12,32,33]. So far, the discussion for the threshold to achieve the highest cooling efficiency is still limited, especially for (sub)tropical areas.

### 1.4. Impact of urban density on cooling performance

The urban morphology, measured by sky view factor (SVF), building height and density, were found to affect the cooling effect of urban greenery. Some studies found that the shading casts by building outweighs the cooling provision by tree shading [34–36]. During the diurnal hours, urban morphology with higher SVF lead to a lower cooling rate and a shorter cooling distance for urban park, and vice versa [10]. It is opposite during the nocturnal periods, cooling effects were more evident in open parks with higher SVF [37]. As for street trees, their cooling effects in low SVF areas were higher than that in high SVF areas [35,36]. In a subtropical city, a study measured 12 pocket parks distributed in areas with different building height and urban density, and found the cooling effects of greenery was not evident in dense areas [18]. In the same city, another study compared cooling benefits of greenery in different urban densities, which revealed the similar conclusion that greenery cooling was higher in lower urban density [38].

### 1.5. Objectives of this study

Based on the above discussion, it was found that there is no consistent conclusion regarding the regression relationship between cooling intensity and greenery coverage; both linear and non-linear patterns were observed and found. In addition, further knowledge in optimal climate regulation and urban greenery planning is needed, especially for subtropical cities. Exploration of greenery cooling efficiency and threshold may facilitate both the understanding of the cooling potential and the implementation of optimal greenery strategies. Considering research methods for current greenery studies, it is difficult to exclude extra impacts and focused only on greenery cooling potential through the observation method. Numerical simulation provides the opportunity to study greenery potential in controlling conditions, yet the intervals for greenery coverage in previous studies were considered too broad to capture potential cooling increment patterns. Besides, the impacts of urban density should also be considered for pedestrian-level thermal comfort improvement. Therefore, the parametric study is conducted to attain three objectives in a subtropical climate background. First, the study aims to investigate whether the cooling efficiency of greenery is in a linear or non-linear pattern. Second, it attempts to examine the impact of urban density and temporal periods in the cooling efficiency pattern. Third, this work seeks to derive a scientific understanding of the cooling efficiency of greenery, which could facilitate appropriate greenery planning and design.

## 2. Materials and method

### 2.1. The study area

Hong Kong, selected for the study area in this work, is situated in the south of the Pearl River Delta on the coast of southern China (located on

22.3193° N, 114.1694° E). Famous for its high building and population density, Hong Kong hosts nearly 7.5 million inhabitants by the end of 2018 [39]. Hong Kong has a humid subtropical climate (Cfa) according to Köppen climate classification, with hot-humid summer months (June to September); average daily temperature is around 28.5 °C and relative humidity of around 80% [40]. The annual mean temperature in territory rises at a rate of 1.2 °C per 100 years [41]. Recent observation reveals intense warming with repeatedly broken temperature records [42]. The government of Hong Kong Special Administrative Region has developed and adopted a series of climatic-responsive design strategies and actions into local planning and design processes [43], and provide and insights for other rapidly densifying cities and regions.

## 2.2. Modeling description and validation

ENVI-met is a numerical simulation model for the complex interactions among surface-plant-atmosphere in different contexts. The model is widely utilized in the urban climate studies, especially for the assessment of microclimate conditions and mitigation strategies, such as greening, cool roof and waterbodies [44,45]. ENVI-met is a grid-based with a fine resolution grid (0.5–10 m) and therefore can assist the studies in local-to micro-scale for their simulations and analysis. As a computational fluid dynamics based model, ENVI-met uses standard  $\kappa-\epsilon$  turbulence model and Reynold Average Navier-Stokes (RANS) equations. This study employs ENVI-met Version 4.3 to perform parametric experiments and simulate the thermal environment.

Regarding urban greenery studies, ENVI-met has been validated and used in different climate backgrounds and research objectives [21,30, 38,46]. Likewise, the model was validated for the present study through a field measurement campaign on 23rd August, 15th and 17<sup>th</sup> October 2016. Two measurement spots were selected and compared: one is under the shade of an *Aleurites moluccana* tree, another is in unshaded open site. Both locations were within a north-south orientation street (Fig. 1 (b) (c)). The TESTO480 instrument was set at 1.5 m height to measure and record air temperature, relative humidity, globe temperature, wind speed (Fig. 1 (d)). The logging interval was 10s sampling. Then 1-h average data was calculated for further analysis. The global temperature was transformed to mean radiant temperature with the following equation [34,47]:

$$MRT = \left[ (T_g + 273.15)^4 + \frac{1.1 * 10^8 * V_a^{0.6}}{\epsilon D^{0.4}} * (T_g - T_a) \right]^{0.25} - 273.15$$

Where:

MRT is mean radiation temperature

$T_g$  is the global temperature

$T_a$  is the air temperature

$V_a$  is the wind speed

$D$  is the diameter of the black globe (= 30 mm)

$\epsilon$  is the emissivity of globe (= 0.95)

## 2.3. Model setting and parametric studies

### 2.3.1. Model initialization

To initialize the parametric model, the meteorological conditions at 23rd August in 2016 (Table 1) were applied to represent a typical summer day in the humid subtropical climate background, based on the assumption that cooling benefits of greenery will be experienced irrespective of the summer condition either typical or extreme [48]. The simulation started at 00:00 and ends at 23:59; however, to allow enough spin-up phase to ensure numerical stability, the data analysis focused between 9:00–18:00.

### 2.3.2. Building configuration

Mong Kok (MK) and Sham Shui Po (SSP) neighborhoods, as the representative high-density districts in Hong Kong (Shown in Fig. 2), were selected to build prototypes for parametric experiments. Characterized by high-density concrete buildings, MK is dominated as compact high-rise (Local Climate Zone LCZ-1) [49], and SSP site is a mixture of compact high-rise (LCZ-1) and compact mid-rise (LCZ-2) [50]. LCZ-1 and LCZ-2, as these neighborhoods, are suffering from high UHI intensity and higher heat stress conditions [35,51]. Referring to the morphological features listed in Table 2, an idealized neighborhood model was developed. The building size is set as 40 × 100 m<sup>2</sup>, while street width is 20 and 32 m, and the building coverage is 44%. Regarding the urban density setting, this study set building heights at 30 m, 60 m, 90 m to represent low-, mid-, and high-urban density conditions distinctively. Although a neighborhood whose building height is 60 m is

**Table 1**  
Model configuration and initialization parameters.

| Items                                 | Input value                  |
|---------------------------------------|------------------------------|
| Simulation day                        | 23 <sup>rd</sup> August 2016 |
| Simulation duration                   | 24 h                         |
| Start time                            | 00:00                        |
| Initial temperature                   | 29.1                         |
| Wind speed at 10 m (m/s)              | 2.83                         |
| Wind direction                        | 220                          |
| Roughness length of the site          | 0.1                          |
| The albedo of road, walls, roof       | 0.3                          |
| Adjustment factor for solar radiation | 0.9                          |
| Cloud cover (Oktas)                   | 2                            |

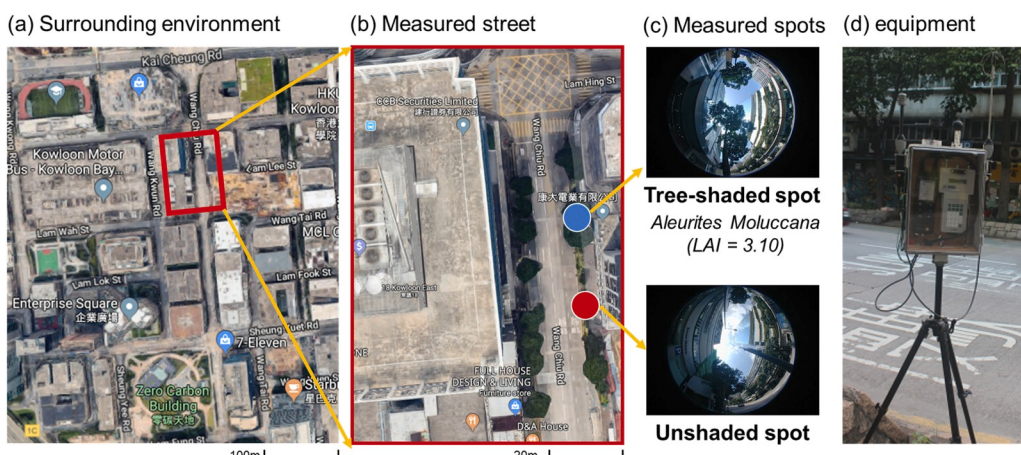


**Fig. 1.** Measurement for model validation.

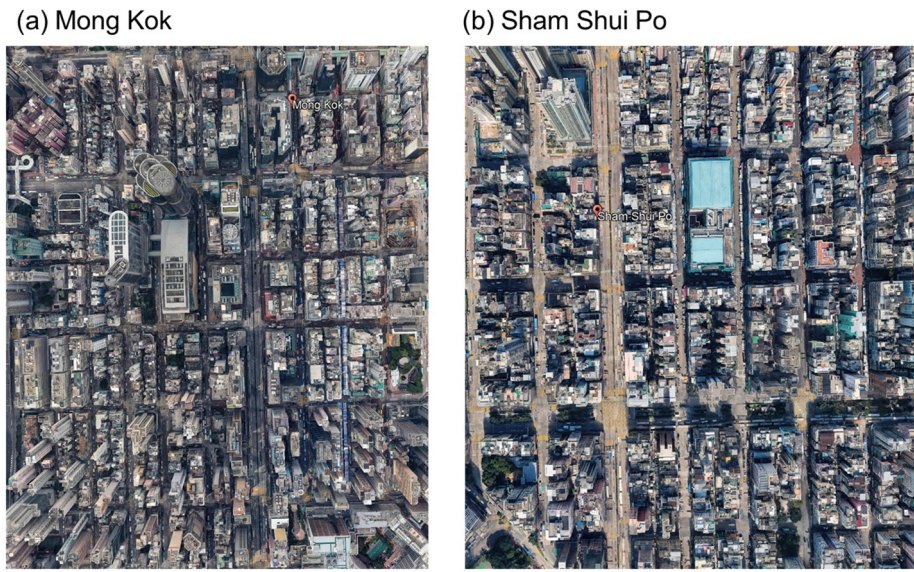


**Fig. 2.** The prototype of building morphology in this study.

deemed as high-density in the most of the cities, this work considers the urban densification trends and takes a forward-looking perspective to discuss greenery cooling benefits in future densified neighborhoods by assuming 60 m height as a mid-density and 90 m as high-density. The simulation domain covers  $680 \times 800 \text{ m}^2$ , which is a domain containing  $170 \times 200$  horizontal grids at 4 m resolution. Vertical grids are set 1 m resolution with 15% telescoping above 2 m building height. 10 nesting grids are added around the main domain to ensure enough space between buildings and model boundary. The basic scheme layout is shown in Fig. 3.

### 2.3.3. Parametric experiments

The parametric experiments were set up for different combinations of urban densities and green coverage ratios. There were 17 scenarios for each urban density group, including one reference scenario and additional 16 different greenery coverage scenarios. The reference scenario consisted of only buildings and street elements without any greenery, while the remaining 16 greenery scenarios were at different coverage ratios, ranging from 2% to 30% at the interval of 2%, as well as whole area coverage (56% coverage other than buildings). This kind of setting is a balance of accuracy and efficiency: on the one hand, 30% greenery coverage is a practical implementation in dense and densifying cities; on the other hand, 2% interval ensure to detect possible trends but avoid too much time consumption for simulations. Besides, the 56% scenario was set to explore the thermal conditions when the whole remaining areas are covered by greenery. Since the objective of this study is focused on greenery coverage and different cooling efficiency, evenly distributed street trees were designed and plant in all greenery scenarios (Shown in Fig. 3 b). Given three groups of urban density (low-, mid-, high-density), there were 51 cases totally in the parametric experiments.

Regarding vegetation features, we have selected *Aleurites moluccana*, which is a typical street tree in residential areas of Hong Kong [52], and one of the top heat mitigator trees [34]. Also, this tree species is plant on the selected field measurement site for validation. To incorporate the

tree species into the idealized neighborhood model, we used the 3D vegetation module ALBERO in ENVI-met to simulate based on the physical characteristics, including tree height (9 m), trunk height (3 m), crown width (7 m), and leaf area index (LAI) ( $2.77 \text{ m}^2/\text{m}^2$ ).

### 2.3.4. Data analysis

Meteorological variables, including air temperature, mean radiant temperature, relative humidity, and wind speed, were imported to the BioMet module of ENVI-met to calculate thermal comfort for every grid point in the study domain at the pedestrian level (1.5 m). In this study, the Physiologically Equivalent Temperature (PET) and Universal Thermal Climate Index (UTCI) were selected out of existing thermal comfort indices, since both of them consider longwave and shortwave radiation that directly affects human thermo-physiologically, especially in the outdoor environment. Although it is found that PET and UTCI perform similarly in humid and subtropical climate for microclimate scale [53], the sensitivity of these two indices to microclimate parameters was shown differently: PET was more sensitive to mean radiant temperature, while UTCI has a higher sensitivity in wind speed and humidity [54]. Therefore, this study included both of them in analysis to explore whether these two indices lead to different patterns for the cooling efficiency of greenery.

In order to avoid boundary effects of the model, further analysis is based on the values of the centered  $118 \times 118$  points or grids in the analysis domain (Red rectangle area in Fig. 3). Then descriptive statistics were used to describe the distribution features of different micro-climate parameters, and different building densities. In addition, both linear and non-linear regression analysis were conducted and compared for heat indicators and greenery coverage ratios. The temporal periods used 9:00–18:00 to represent daytime when the solar radiation could largely influence thermal comfort conditions and may even cause pedestrian's discomfort and heat stress.

## 3. Results and analyses

### 3.1. Model validation result

Fig. 4 showed the correlation analysis results for the measurement-based results and simulation results in terms of air temperature (AT) and mean radiant temperature (MRT). For both tree-shaded and unshaded points, the coefficients of determination ( $R^2$ ) for AT and MRT were  $R^2 = 0.79\text{--}0.81$  and  $R^2 = 0.7\text{--}0.74$  respectively. The

**Table 2**  
Morphological features in MK and SSP blocks.

| Morphological features  | Mong Kok | Sham Shui Po |
|-------------------------|----------|--------------|
| Urban density           | 43%      | 41%          |
| Average building height | 32 m     | 26 m         |
| Main street width       | 36 m     | 31 m         |
| Average street width    | 18–20 m  | 18–20 m      |

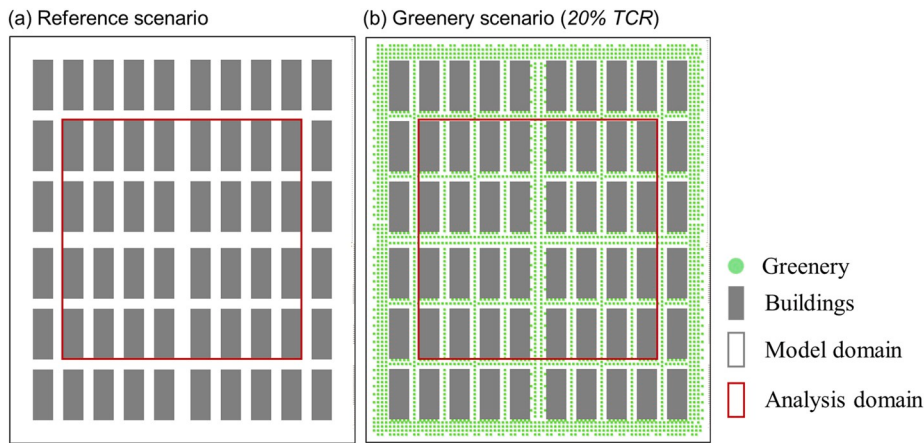


**Fig. 3.** Model schematic layout and scenarios examples (Building coverage ratio = 44%).

underestimation of AT may be due to anthropogenic heat in the measurement area but not accounted for in the model, while the overestimation of MRT may be owing to the static setting for cloud conditions and radiation adjustment factor. Previous studies have also evaluated the model's ability for urban greenery strategies [35,36,38, 55]. In those studies, correlation coefficients between measured and modeled results were 0.63–0.92 for AT and 0.7–0.99 for MRT. Based on these, we concluded that ENVI-met is a reliable tool to estimate the cooling effects of urban greenery for the research purpose in this study.

### 3.2. Thermal characteristics of the reference scenarios

The thermal features of the reference scenarios were presented and discussed firstly in this section. Values were extracted from the centered  $118 \times 118$  points or grids for heat indicators, including AT, MRT, Physiologically Equivalent Temperature (PET), and Universal Thermal Climate Index (UTCI). Fig. 5 is the ridge plots describing frequency distributions for different diurnal hours for mid-density neighborhood. AT ranges from 27 to 33 °C with a single-ridge distribution. The range was wider for MRT, spanning from 20 to 60 °C. Two ridges were observed for MRT during daytime except at 18:00 when the global direct radiation had been greatly attenuated at dusk hour. The distance between the two ridges was found to be shortest at 12:00–13:00 LST (Local solar time) and the longest at 9:00 and 16:00 LST. Moreover, although the highest MRT was detected during 14:00–16:00 LST, the second ridge with higher temperature had higher frequency during 12:00–13:00 LST. This means the highest temperature appears at 14:00–16:00 LST, but more areas within the neighborhood were with higher MRT at 12:00–13:00 LST. In addition, the distance between two ridges within 1

h was around 10–20 °C, even larger than the discrepancy between hours. This indicated that MRT in the reference scenarios had higher variance spatially (within 1 h) than temporally (between hours). Largely affected by MRT, PET and UTCI showed a similar pattern with two ridges. The values of PET and UTCI ranged in 25–45 °C and 28–40 °C respectively, which was both wider than AT, but narrower than MRT.

As for low- and high-density cases, a similar temporal pattern was observed although with different temperature values (Shown in Figs. S2 and S3 in Supplementary File). To determine whether there were differences in the heat indicators accordingly, whilst the independent group is urban density, multivariate analysis of variance (MANOVA) was applied to test. Results (Table A1 in Appendix A) show that the *f*-value was greater than *f*-critical values as the alpha level at 0.001, and *p*-values were all less than 0.001. Thus, the null hypothesis was rejected, which suggests significant differences for targeted heat indicators between groups of urban densities.

To show the distribution of overall frequency among three urban densities, the cumulative frequency profiles for each heat indicator were presented in Fig. 6. In general, values observed in the low-density neighborhoods were higher, while the lowest was observed in the high-density. This indicated that a high-density urban morphology might moderate overheating by providing shading, which was also found in previous studies [56]. As for different heat indicators, the difference in AT was stable among the three densities groups, since the intervals between each line were similar as temperature rises. This indicates a negligible heterogeneity in thermal conditions among urban densities. However, for MRT, PET, and UTCI, values in low-density showed a higher increasing rate than that of mid- and high-density. Especially in the cumulative frequency range of [0.25, 0.75], differences between

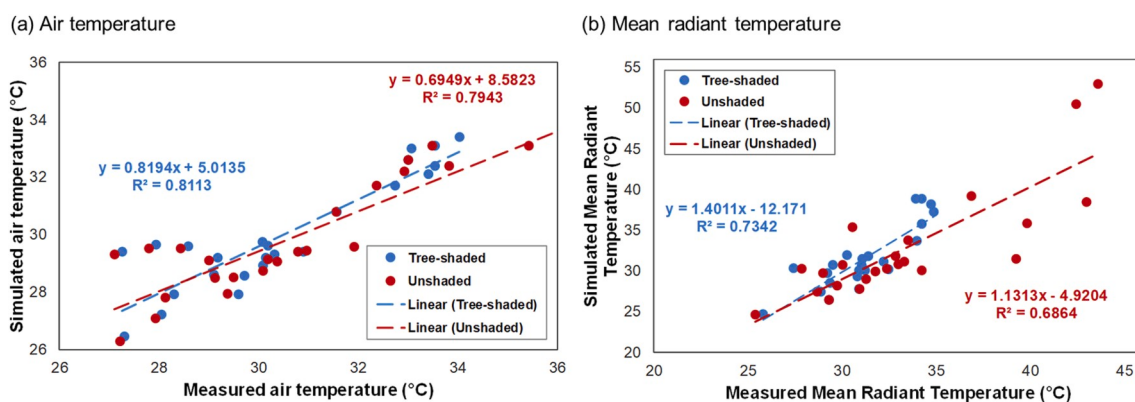


**Fig. 4.** Relationship between simulation and measurement for (a) air temperature, (b) mean radiant temperature (Data for 9:00–17:00 local time on 23rd Aug, 15th and 17th Oct 2016).

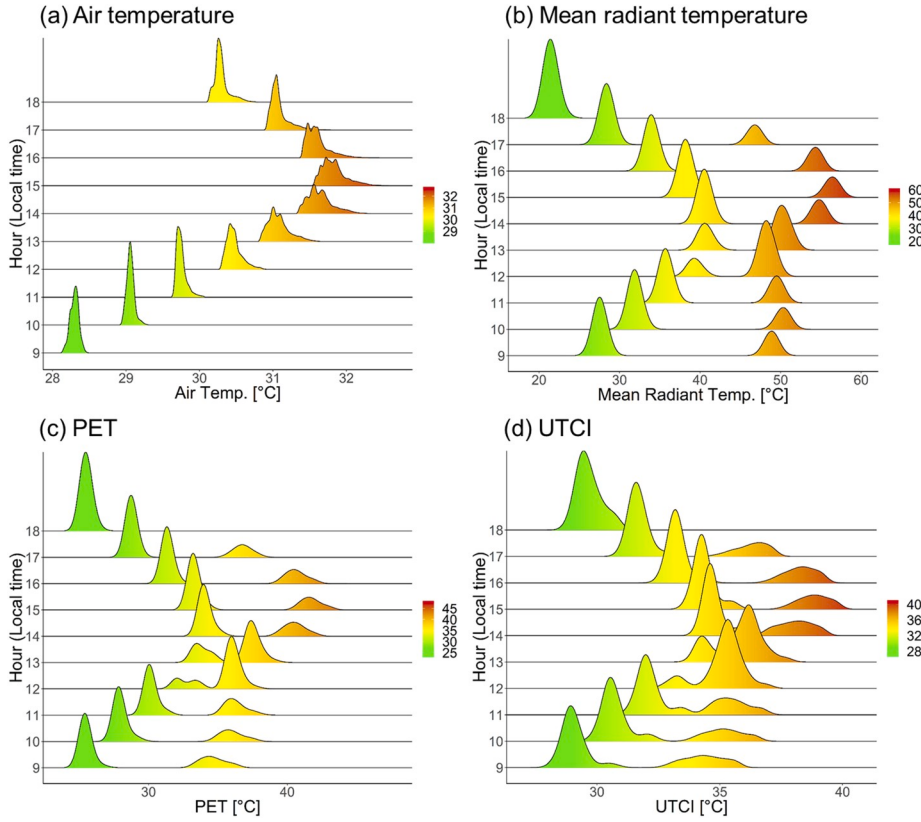


**Fig. 5.** Ridge plot of hourly frequency distribution pattern for the four heat indicators (60 m Mid-density).

low- and mid-density groups were gradually over 2 times and nearly 3 times than the difference between mid- and high-density groups. These results are in accordance with a previous study where high-density environments were found to benefit from shadings of buildings [57].

### 3.3. Tree coverage ratios and cooling benefits

In this section, the cooling benefits were discussed in various tree coverage ratios (TCR), where cooling benefits were defined as the difference between each greenery scenario and the corresponding reference scenario for three urban density settings. Mid-density cases were illustrated in this section while the impacts of urban densities in the cooling benefits were discussed in the following section (Section 4.4). To demonstrate the spatial distributions of the cooling benefits, Fig. 7 shows the cooling effects of 2%, 10%, 20%, and 56% TCR during the hottest hour (15:00). The cooling distribution was spatially heterogeneous, and more cooler areas were found in the North-East corner where is the downwind direction in ENVI-met simulation setting. This was explained by other studies that the downwind areas benefit the most from greenery [36,58]. Regarding different indicators, the spatial distribution for AT was generally smoother, while the spatial diversity was higher for MRT, PET, and UTCI. Furthermore, UTCI at 2% TCR case showed higher spatial diversity than the other heat indicators. This may be because UTCI is sensitive to thermal stimuli [53].

According to the results in Section 3.2, two temporal periods were selected for the following analysis, i.e. daytime (09:00–18:00) and hottest periods (14:00–16:00). Shown in Fig. 8, the cooling benefits were presented for these two periods in their quartiles. Generally, increasing TCR leads to higher cooling benefits for both periods. And the cooling magnitude during the hottest period was greater than that of daytime period. As introducing more trees, AT and MRT in the whole analysis domain were decreased. However, for PET and UTCI, slightly increasing temperature was observed in a small fraction of areas, where the cooling

benefits were positive values. This could be explained that the wind speed was slowed down and the relative humidity was increased by trees (Fig. S8 in Supplementary File).

In terms of median (middle values), the cooling benefits of AT reached 0.8 °C for daytime and 1 °C for the hottest period when TCR was 56%. As for MRT, PET, and UTCI, little disparity was observed between two periods; while the medium cooling benefits were around 7 °C, 2.5 °C, and 1 °C respectively. Regarding ranges of cooling benefits, wider ranges were noticed for MRT, PET, and UTCI, but a smaller range for AT. Additionally, when TCR increased, larger ranges of MRT, PET, and UTCI were identified for both periods and AT for the daytime period. To be specific, the cooling ranges of AT in the daytime gradually increased with enlarging TCR, and the range in the hottest period had no apparent change. But for MRT and PET, it is interesting to detect the cooling range abruptly expanded at 8% TCR in the daytime and at 20% TCR during the hottest period. As for UTCI, only abrupt expansion was found for 20% TCR during the hottest period. This implied that evident cooling effects appeared in 8% of TCR for daytime, and in 20% of TCR for hottest periods.

### 3.4. Urban density and cooling benefits

This section intended to furtherly discuss the impacts of urban density in cooling benefits from trees. Shown in Fig. 9, the cooling benefits were compared under the three urban density scenarios and two selected temporal periods. Generally, given the same TCR, the cooling benefits from greenery were greatest in low-density neighborhood, followed with mid- and high-density neighborhoods; and this result was consistent with both temporal periods. This finding resonated with that of previous studies [34,38]. In terms of different heat indicators, for AT, MRT, and PET, the cooling provision by greenery was ranked from the highest to lowest as: low-, mid-, and high-density neighborhoods. But for UTCI, the cooling benefits were almost at the same level for both mid-

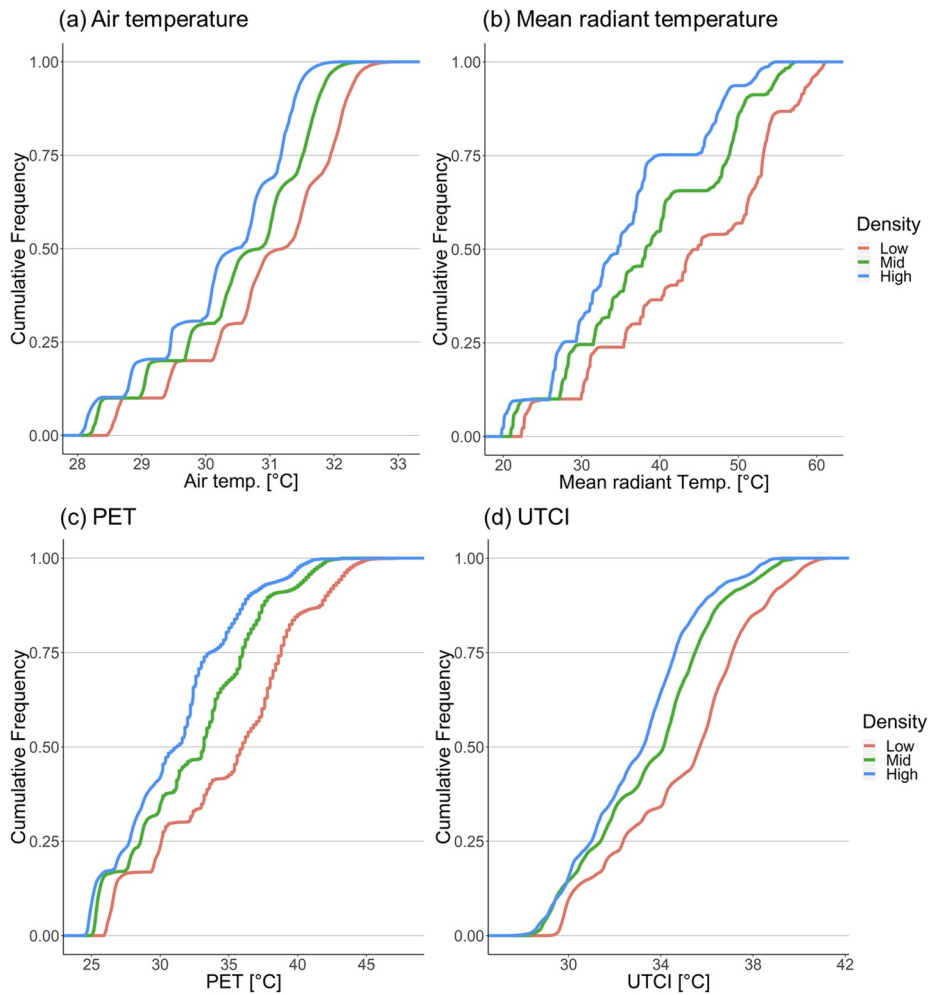


**Fig. 6.** Cumulative frequency plot of low, mid, high urban density for the four heat indicators.

and high-density cases based on medium values. Moreover, AT and UTCI were only slightly affected by densities, as little differences were observed between mid- and high-density neighborhoods. MRT was detected to be the most sensitive parameter towards urban density, since the discrepancy between different density groups were the largest.

As for the cooling benefits in the daytime periods, the ranges of the cooling benefits in AT were  $[-1.40, 0.00]$  °C,  $[-1.34, 0.01]$  °C,  $[-1.23, 0.03]$  °C for low-, mid- and high-density respectively, and  $[-5.79, 1.74]$  °C,  $[-5.74, 2.03]$  °C,  $[-4.60, 2.41]$  °C for UTCI. MRT had the largest ranges in  $[-23.69, 0.00]$  °C,  $[-22.79, 0.00]$  °C,  $[-21.82, 0.00]$  °C for low-, mid- and high-density separately. PET was largely affected by MRT, showing thermal benefits of  $[-13.80, 4.00]$  °C,  $[-12.30, 4.20]$  °C,  $[-12.51, 2.40]$  °C for low-, mid- and high-density distinctively. During the hottest time, MRT, PET, and UTCI had almost the same ranges with those of the daytime period. But for AT, narrower ranges yet larger cooling magnitudes were found, whose ranges were  $[-1.27, -0.01]$  °C,  $[-1.16, 0.00]$  °C,  $[-1.12, 0.02]$  °C for low, mid- and high density individually.

Furthermore, comparing the selected two temporal periods, urban density affected the greenery cooling effects to varying extents. On the whole, the cooling difference by urban density was larger in the hottest period than that in the daytime. This implied that urban density had a higher impact in the greenery cooling during the hottest periods. Based on different heat indicators, MRT was the most sensitive indicator towards urban density, irrespective of two temporal periods. Especially, MRT showed extremely limited cooling benefits in the high-density cases during the hottest time, which was totally different from the

daytime. Similar to MRT, PET showed a moderately different response towards density variations between these two periods, but for UTCI, these responses towards density variations seemed to be similar between the two periods. In addition, abrupt expansions of ranges were observed for MRT, PET, and UTCI during the two periods, which were summarized in Table 3. AT seemed to vary smoothly and gradually. In Table 3, the abrupt expansion of cooling ranges appeared in low TCR for low-density and higher TCR for mid- or high-density. For PET and UTCI, there was even no expansion point of cooling for high-density, which means the cooling from greenery was limited by buildings. The abrupt expansion means certain TCR lead to apparent cooling benefits and spatial heterogeneity for thermal distributions.

### 3.5. Pattern of cooling efficiency and coverage threshold

In order to track the trend of cooling efficiency, the regression analysis was conducted between different TCRs and cooling benefits. Two different regression models (linear and non-linear) were compared for two selected temporal periods (See Fig. 10). In general, the coefficient of determination  $R^2$  was higher in the logarithm regression than in the linear regression for four heat indicators, despite of different urban densities and temporal periods. Regarding the variations in urban density and temporal periods, the main variance was the cooling magnitude, which has been illustrated in Section 4.3 and 4.4. In addition, for each pair of linear and logarithm regression, two-interception points can be observed. When TCR was between 8 and 36%, the linear regression overestimated the cooling benefits of urban greenery; while in the lower

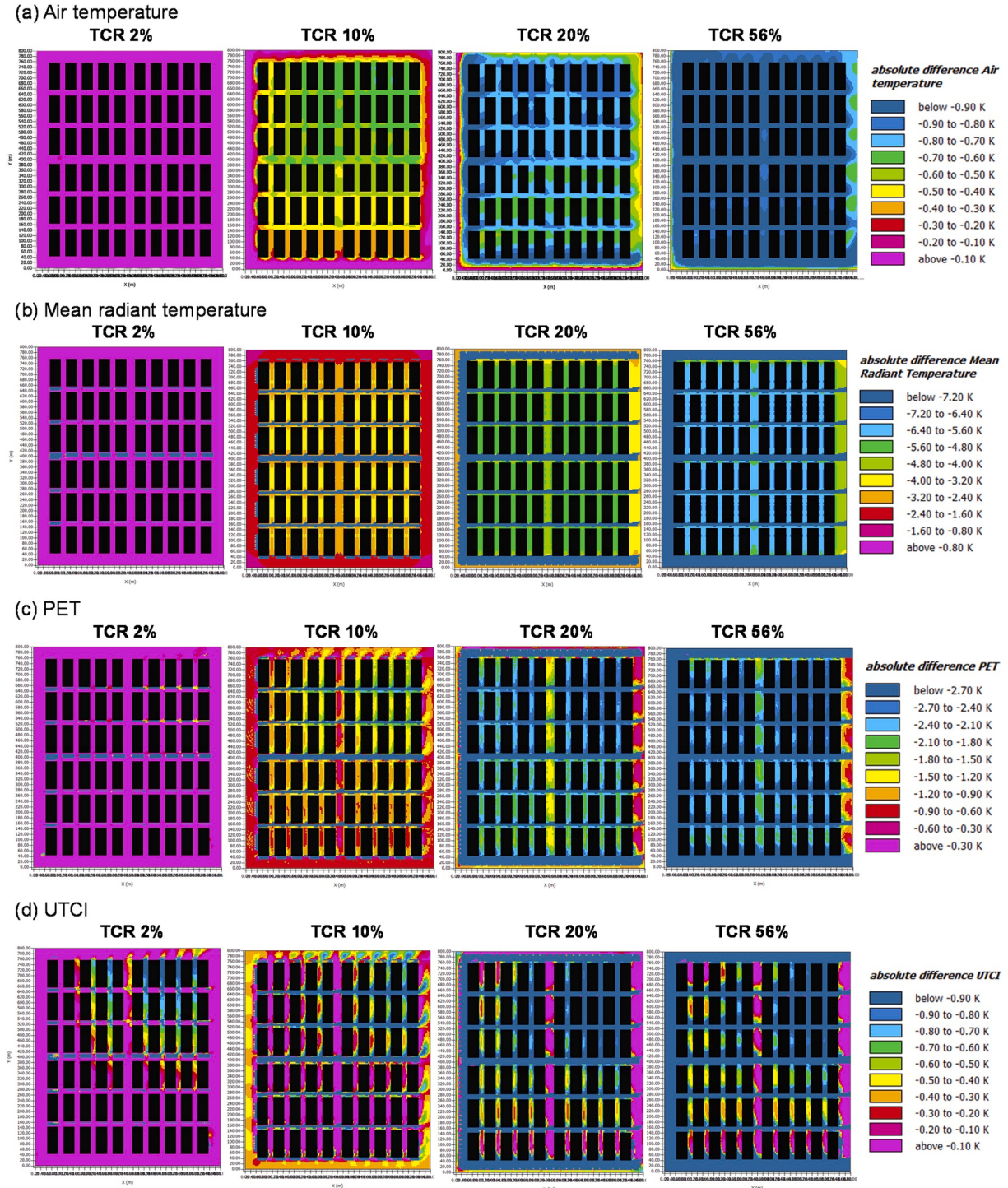


**Fig. 7.** Spatial distributions of cooling benefits for the four heat indicators (GCR: 2%, 10%, 20% and 56%, Time: 15:00, Mid-density).

and upper ranges of TCR, it underestimated the cooling beneficial than the logarithm pattern. Regarding different urban density cases, the overestimation ranges were slightly broader in the low-density neighborhoods.

In terms of different heat indicators, cooling efficiency measured by AT, MRT and PET were apparently in the logarithm pattern. But for UTCI, the logarithm regression ( $R^2$ : 0.74–0.8) seemed to have a slightly higher R-square than the linear regression ( $R^2$ : 0.54–0.7). Except for mid-density during the hottest period, the two regressions ( $R^2$ : 0.74 vs. 0.7) seemed little difference. The inconsistency between PET and UTCI in the cooling efficiency might be because PET was more sensitive in

higher temperature compared to UTCI [40]. Although the logarithm pattern of UTCI performs not as well as three other indicators, the UTCI values showed little increments and exhibited minor fluctuations in the higher end of TCR.

Given the trends in logarithm, the cooling benefits from greenery do not increase continuously with increasing TCR. Generally, the cooling rate slowed significantly at 20% TCR and was almost stable at 30% TCR. Though the whole area was covered by the tree canopy (56% TCR), the cooling benefits showed no apparent improvement compared with the thermal conditions in 30% TCR. Especially for the two thermal comfort indices, PET and UTCI, the cooling benefits present minor variations

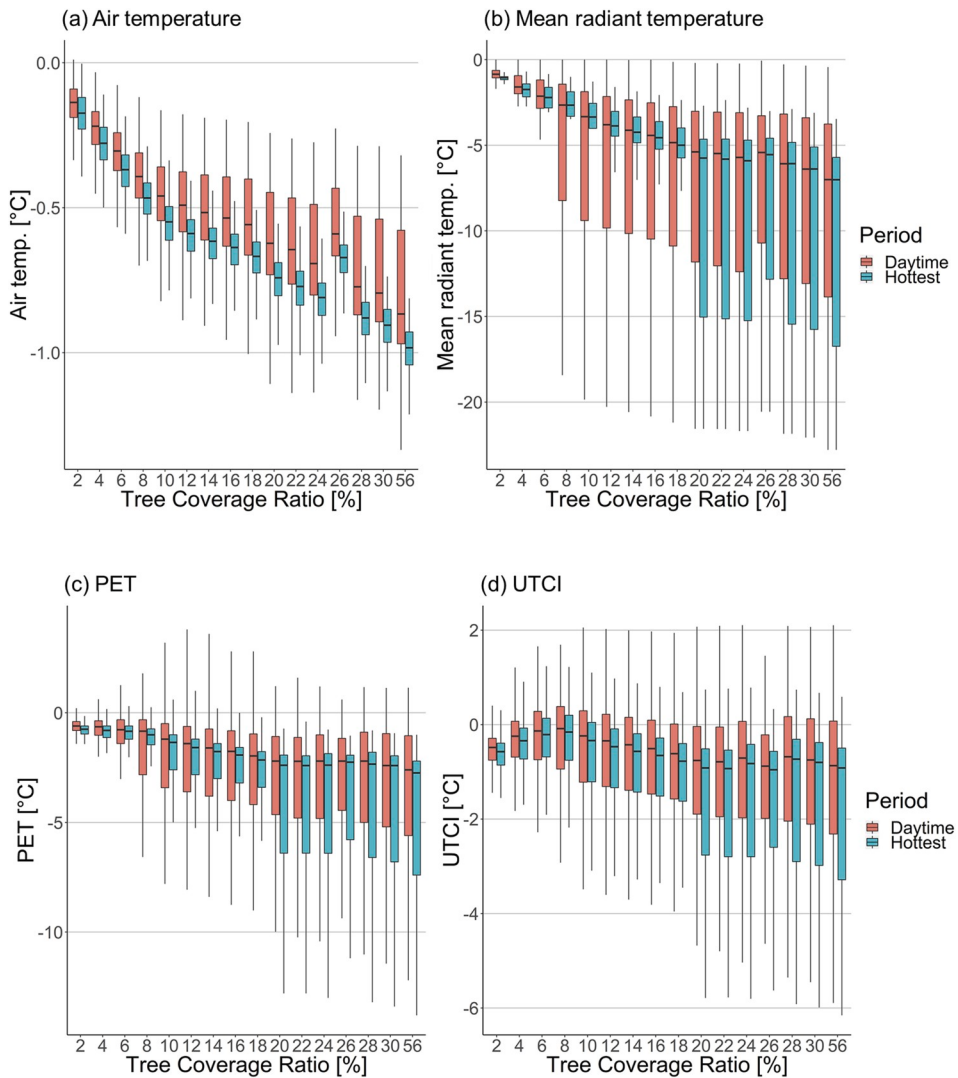


**Fig. 8.** Cooling benefits with different TCR in the daytime and hottest periods for the four heat indicators (Mid-density).

from 20% TCR and above. Therefore, the findings demonstrated that the cooling efficiency of trees reached its peak at 20–30% TCR, as increasing TCR does not lead to obvious cooling improvement. Although the urban density affected the cooling magnitude from greenery; the lower density, the higher cooling benefits, the cooling efficiency of trees is consistent under different urban density scenarios when the optimal TCR was at 20–30%.

#### 4. Discussion and impacts of the study

Based on the findings from this study, the relationship between the cooling effect and TCR is non-linear, which does not totally agree with the general assumption that “the more greening, the cooler for our built environment”. We opined that this general assumption might be true for other climate but not in the sub-tropical hot-humid climate, where 20–30% coverage ratio was found to be the most efficient and effective threshold for cooling provision. This finding corroborates with that of a study conducted in a dozen North American cities, showing the cooling potential increases sharply with the introduction of greening, and then levels off when vegetated fraction reaches 20–30% [28]. However, more studies about threshold recommendations suggested that the greenery threshold for different cities and different seasons is non-identical. Cities in North America, Europe, Africa, and Asia were studied for energy fluxes and its seasonal variations; this study detected an overall 43%

threshold for vegetated fraction but this value changed along with climate background and seasons [59]. The thresholds also vary based on different implementation scales. For instance, at the city scale, the threshold value of efficiency (TVoE) of urban greenery was introduced and analyzed for different Asian cities, and conclusions were given that optimal greenspace area was 0.92–0.96 ha for the cities with rich vegetation and 0.6–0.62 ha for the cities with low vegetation quantity [1,60]. At block scale, a 40% coverage ratio in greenery was recommended for a midsize and Midwest city in the USA, considering the greatest marginal increase in cooling benefits [24]. Therefore, more researches are expected to discuss the impact factors of cooling efficiency and thresholds. This kind of investigation and discussion can assist urban planners and managers to make use of land resources and optimize the cooling and other potential beneficial of urban greenery. Other than the thermal environment, the coverage threshold for greenery has also been discussed in other perspectives. For example, tree coverage and landscape preference were explored and a threshold value for tree cover density was found to be 41% to ensure a moderate preference in U.S Midwestern urban areas [61]. Thus, a thorough analysis and discussion is expected to promote explicit environmental planning and greenery design in the future.

With prominent problems in increasing ambient temperature and deteriorating outdoor thermal comfort, urban greenery should be provided both in quantity and quality [62]. Current policies and guidelines

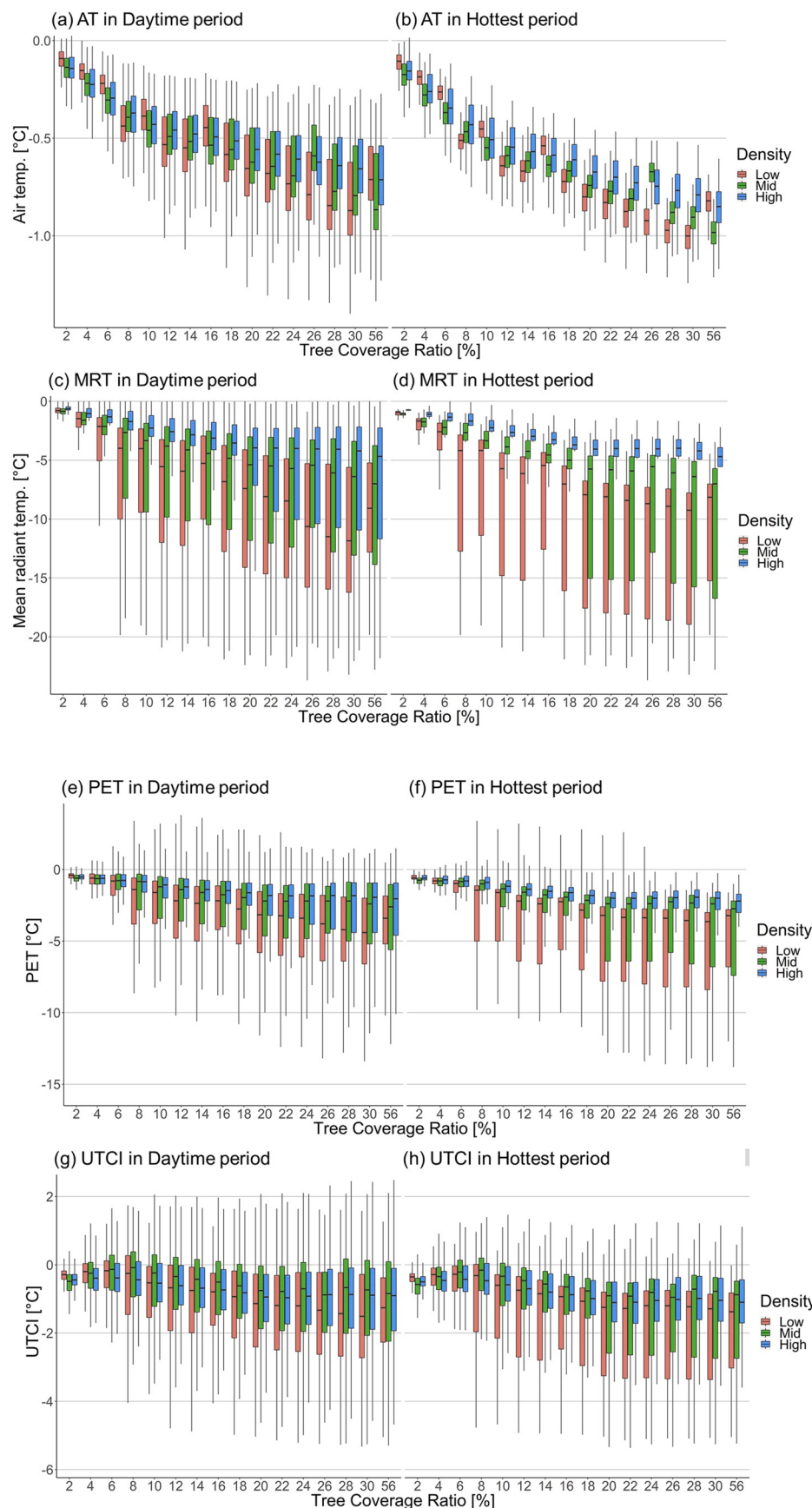


**Fig. 9.** Cooling benefits with different urban densities in the daytime and hottest periods for the four heat indicators.

**Table 3**

TCR for abrupt expansion of cooling ranges (Based on information in Fig. 9).

| Heat indicator | Urban density | Daytime | Hottest period |
|----------------|---------------|---------|----------------|
| AT             | Low           | N       | N              |
|                | Mid           | N       | N              |
|                | High          | N       | N              |
| MRT            | Low           | 8%      | 8%             |
|                | Mid           | 8%      | 20%            |
|                | High          | 20%     | N              |
| PET            | Low           | 8%      | 8%             |
|                | Mid           | N       | 20%            |
|                | High          | N       | N              |
| UTCI           | Low           | 8%      | 8%             |
|                | Mid           | N       | 20%            |
|                | High          | N       | N              |

\*Where N represents no apparently abrupt changes.

in Hong Kong provided no quantitative prescription and considered little in environmental benefits [38]. For instance, Greening Master Plan (GMP) provided strategies for urban districts with planting species, locations, and themes [63]. In addition, Hong Kong planning standards and guidelines suggest 20–30% greenery coverage for individual sites [64]. These suggestions are mainly based on considerations in both practical feasibilities, and the aesthetic and recreational functions. The results of this study support this regulation from a climate and efficiency perspective. It is worth to mention that the result of this study is confined in a humid subtropical climate, other cities should carefully refer to the results of the threshold limitations. The methodology and flowchart, however, could provide some experience for other cities.

## 5. Conclusions and future research works

This study investigated the cooling efficiency and compared two regression patterns (both linear and non-linear) at a neighborhood scale. Parametric studies were conducted in a validated ENVI-met model for various greenery coverage ratios, three different urban densities, and two temporal periods in typical summer day. Four heat indicators and

thermal comfort indices were taken to measure the cooling benefits of greenery. Regardless of heat indicators, urban densities, and temporal periods, greenery coverage ratio and their cooling benefits were found to be related non-linearly in a logarithm pattern. This curve relationship indicated that greenery cooling efficiency increases at the lower end of greenery coverage ratio, then decrease as greenery abundance increase, and reached the highest at 20–30%. Above the 30% coverage ratio, the marginal cooling benefits nearly levelled off. This understanding could be directly applied to other sub-tropical cities with LCZ 1 and 2 urban morphological characteristics. Furthermore, the findings could be used to efficiently improve the green master plan and design control for creating better microclimatic conditions and achieving thermal comfort at the pedestrian level in urban areas, especially for cities with limited land resources and high-density development needs.

Some limitations need to be clarified for a better understanding of the results. First, this study applied single tree species in evenly spatial distribution, which is the ideal situations instead of a real one. Although LAI and height width were used as the basic input, other tree species with similar features can also refer to the results of this study, future studies are expected to explore the impact of different species and various spatial distributions. Second, analysis periods were focused on diurnal time. As the UHI intensity peak appears in the nighttime, further studies could also explore nocturnal patterns and compare its difference with daytime periods. Lastly, the urban density was measured by building height with certain building coverage. Other factors of urban morphology, such as different sky view factor or aspect ratios, and different road orientations may need further studies. In future, the same method in this study could be adopted in other climate regions and different seasons. Sensitivity in the variation of wind speed and direction is another interesting direction worth further examination.

## Declaration of competing interest

None.

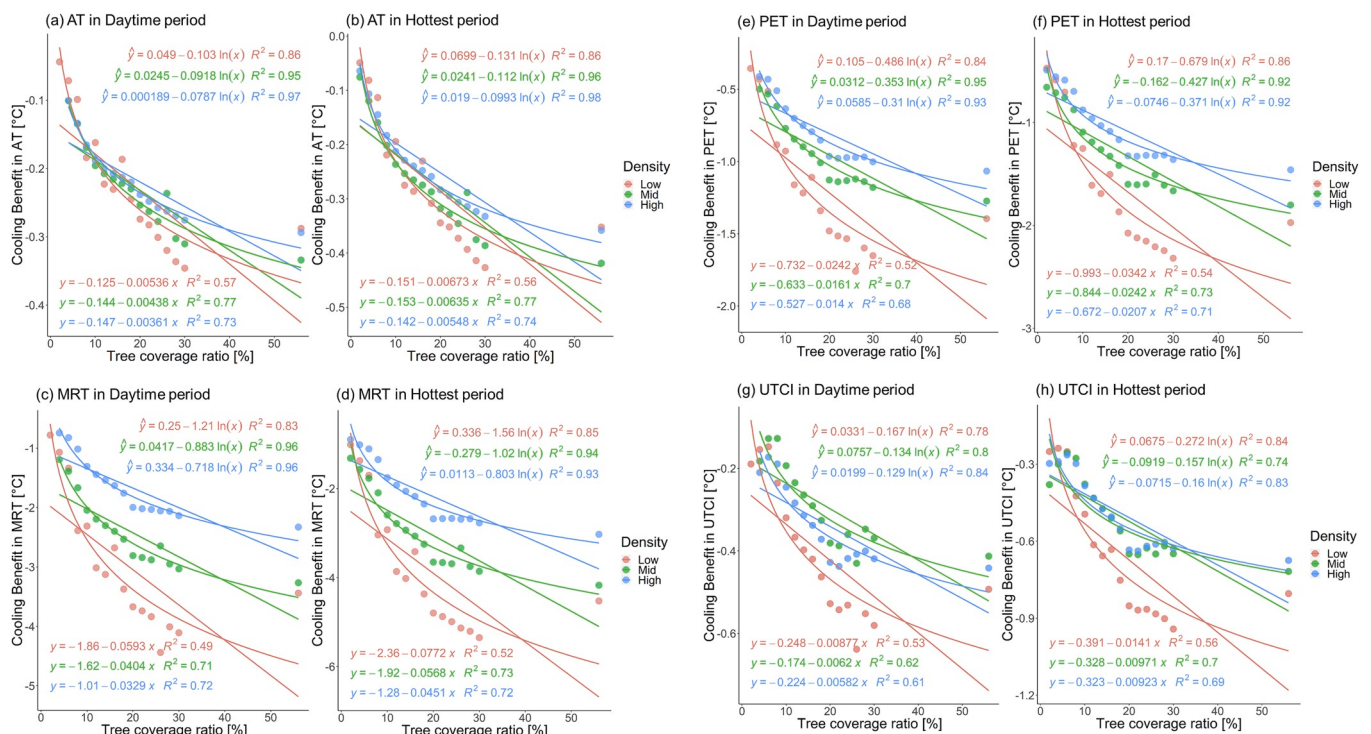


Fig. 10. Cooling efficiency patterns in linear and non-linear regression in daytime and hottest periods for the four heat indicators.

## Acknowledgements

This study is supported by a postgraduate studentship and the “Vice-Chancellor’s Discretionary Fund” of the Chinese University of Hong Kong.

## Appendix B. Supplementary data

Supplementary data to this article can be found online at <https://doi.org/10.1016/j.buildenv.2020.106772>.

## Appendix A

**Table A1**  
MANOVA analysis result of tree-free cases

|                | Response | AT           |            |             |        |
|----------------|----------|--------------|------------|-------------|--------|
|                | Df       | Sum Sq       | Mean Sq    | F value     | Pr(>F) |
| Density        | 1        | 14352.02     | 14352.02   | 11484.32    | 0.00   |
| Residuals      | 176355   | 220391.81    | 1.25       |             | ***    |
|                | Response | MRT          |            |             |        |
|                | Df       | Sum Sq       | Mean Sq    | F value     | Pr(>F) |
| Density        | 1        | 2116870.20   | 2116870.20 | 19969.64    | 0.00   |
| Residuals      | 176355   | 18694409.13  | 106.00     |             | ***    |
|                | Response | PET          |            |             |        |
|                | Df       | Sum Sq       | Mean Sq    | F value     | Pr(>F) |
| Density        | 1        | 454216.95    | 454216.95  | 19610.12    | 0.00   |
| Residuals      | 176355   | 4084799.64   | 23.16      |             | ***    |
|                | Response | UTCI         |            |             |        |
|                | Df       | Sum Sq       | Mean Sq    | F value     | Pr(>F) |
| Density        | 1        | 119314.58    | 119314.58  | 15244.67    | 0.00   |
| Residuals      | 176355   | 1380267.18   | 7.83       |             | ***    |
|                | Response | RH           |            |             |        |
|                | Df       | Sum Sq       | Mean Sq    | F value     | Pr(>F) |
| Density        | 1        | 216495.42    | 216495.42  | 9893.53     | 0.00   |
| Residuals      | 176355   | 3859092.04   | 21.88      |             | ***    |
|                | Response | WS           |            |             |        |
|                | Df       | Sum Sq       | Mean Sq    | F value     | Pr(>F) |
| Density        | 1        | 1908.36      | 1908.36    | 14102.55    | 0.00   |
| Residuals      | 176355   | 23864.39     | 0.14       |             | ***    |
| —              |          |              |            |             |        |
| Signif. codes: | ***      | <b>0.001</b> | **         | <b>0.01</b> |        |
|                | **       | <b>0.05</b>  | *          | <b>0.1</b>  |        |

## References

- [1] Z. Yu, et al., How can urban green spaces be planned for climate adaptation in subtropical cities? *Ecol. Indicat.* 82 (2017) 152–162.
- [2] T.U.o.H.K. The Kadoorie Institute, Hong Kong’s Vulnerability to Global Climate Change Impacts an Oxfam Report on 2010 Public Survey and Policy Recommendations, 2010.
- [3] H. Akbari, M. Pomerantz, H. Taha, Cool surfaces and shade trees to reduce energy use and improve air quality in urban areas, *Sol. Energy* 70 (3) (2001) 295–310.
- [4] T.E. Morakinyo, et al., Estimates of the impact of extreme heat events on cooling energy demand in Hong Kong, *Renew. Energy* 142 (2019) 73–84.
- [5] R.L. Wilby, Constructing climate change scenarios of urban heat island intensity and air, *Qual. Environ. Plann. B: Plann. Design* 35 (5) (2008) 902–919.
- [6] O. Buchin, et al., Evaluation of the health-risk reduction potential of countermeasures to urban heat islands, *Energy Build.* 114 (2016) 27–37.
- [7] A. Middel, E.S. Krayenhoff, Micrometeorological determinants of pedestrian thermal exposure during record-breaking heat in Tempe, Arizona: introducing the MaRTy observational platform, *Sci. Total Environ.* 687 (2019) 137–151.
- [8] K.W. Robert, T.M. Parris, A.A. Leiserowitz, What is sustainable development? Goals, indicators, values, and practice, *Environment* 47 (3) (2005) 8–21.
- [9] B. Stone, Urban heat and air pollution: an emerging role for planners in the climate change debate, *J. Am. Plann. Assoc.* 71 (1) (2005) 13–25.
- [10] H. Upmanis, I. Eliasson, S. Lindqvist, The influence of green areas on nocturnal temperatures in a high latitude city (Göteborg, Sweden), *Int. J. Climatol.* 18 (6) (1998) 681–700.
- [11] C.R. Chang, M.H. Li, S.D. Chang, A preliminary study on the local cool-island intensity of Taipei city parks, *Landscl. Urban Plann.* 80 (4) (2007) 386–395.
- [12] L. Shashua-Bar, D. Pearlmuter, E. Erell, The cooling efficiency of urban landscape strategies in a hot dry climate, *Landscl. Urban Plann.* 92 (3) (2009) 179–186.
- [13] G.L. Feyisa, K. Dons, H. Meilby, Efficiency of parks in mitigating urban heat island effect: an example from Addis Ababa, *Landscl. Urban Plann.* 123 (2014) 87–95.
- [14] D.E. Bowler, et al., Urban greening to cool towns and cities: a systematic review of the empirical evidence, *Landscl. Urban Plann.* 97 (3) (2010) 147–155.
- [15] S.W. Myint, et al., The impact of distinct anthropogenic and vegetation features on urban warming, *Landscl. Ecol.* 28 (5) (2013) 959–978.
- [16] Z. Ren, et al., Estimation of the relationship between urban park characteristics and park cool island intensity by remote sensing data and field measurement, *Forests* 4 (4) (2013) 868–886.
- [17] X. Cao, et al., Quantifying the cool island intensity of urban parks using ASTER and IKONOS data, *Landscl. Urban Plann.* 96 (4) (2010) 224–231.
- [18] P. Lin, et al., Effects of urban planning indicators on urban heat island: a case study of pocket parks in high-rise high-density environment, *Landscl. Urban Plann.* 168 (2017) 48–60.
- [19] S. Hamada, T. Ohta, Seasonal variations in the cooling effect of urban green areas on surrounding urban areas, *Urban For. Urban Green.* 9 (1) (2010) 15–24.
- [20] H. Yan, F. Wu, L. Dong, Influence of a large urban park on the local urban thermal environment, *Sci. Total Environ.* 622–623 (2018) 882–891.

- [21] A. Middel, N. Chhetri, R. Quay, Urban forestry and cool roofs: assessment of heat mitigation strategies in Phoenix residential neighborhoods, *Urban For. Urban Green.* 14 (1) (2015) 178–186.
- [22] B. Szulczecka, et al., How much green is needed for a vital neighbourhood? In search for empirical evidence, *Land Use Pol.* 38 (2014) 330–345.
- [23] M.V. Monteiro, et al., The impact of greenspace size on the extent of local nocturnal air temperature cooling in London, *Urban For. Urban Green.* 16 (2016) 160–169.
- [24] C.D. Ziter, et al., Scale-dependent interactions between tree canopy cover and impervious surfaces reduce daytime urban heat during summer, *Proc. Natl. Acad. Sci. U. S. A.* 116 (15) (2019) 7575–7580.
- [25] Z. Wu, P. Dou, L. Chen, Comparative and combinative cooling effects of different spatial arrangements of buildings and trees on microclimate, *Sustainable Cities and Society* 51 (2019) 101711.
- [26] T.F. Zhao, K.F. Fong, Characterization of different heat mitigation strategies in landscape to fight against heat island and improve thermal comfort in hot-humid climate (Part II): evaluation and characterization, *Sustain. Cities Soc.* 35 (2017) 841–850.
- [27] A. Middel, et al., Land cover, climate, and the summer surface energy balance in Phoenix, AZ, and Portland, OR, *Int. J. Climatol.* 32 (13) (2011) 2020–2032.
- [28] C.S.B. Grimmond, T.R. Oke, Turbulent heat fluxes in urban areas: observations and a local-scale urban meteorological parameterization scheme (LUMPS), *J. Appl. Meteorol.* 41 (7) (2002) 792–810.
- [29] D. Pearlmuter, E.L. Krüger, P. Berliner, The role of evaporation in the energy balance of an open-air scaled urban surface, *Int. J. Climatol.* 29 (6) (2008) 911–920.
- [30] Z. Wu, L. Chen, Optimizing the spatial arrangement of trees in residential neighborhoods for better cooling effects: integrating modeling with in-situ measurements, *Landsc. Urban Plann.* 167 (2017) 463–472.
- [31] C. Skelhorn, S. Lindley, G. Levermore, The impact of vegetation types on air and surface temperatures in a temperate city: a fine scale assessment in Manchester, UK, *Landsc. Urban Plann.* 121 (2014) 129–140.
- [32] J. Yang, E. Bou-Zeid, Scale dependence of the benefits and efficiency of green and cool roofs, *Landsc. Urban Plann.* 185 (2019) 127–140.
- [33] P. Gober, et al., Tradeoffs between water conservation and temperature amelioration in Phoenix and portland: implications for urban sustainability, *Urban Geogr.* 33 (7) (2012) 1030–1054.
- [34] T.E. Morakinyo, et al., A study on the impact of shadow-cast and tree species on in-canyon and neighborhood's thermal comfort, *Build. Environ.* 115 (2017) 1–17.
- [35] Z. Tan, K.K.-L. Lau, E. Ng, Planning strategies for roadside tree planting and outdoor comfort enhancement in subtropical high-density urban areas, *Build. Environ.* 120 (2017) 93–109.
- [36] Z. Tan, K.K.-L. Lau, E. Ng, Urban tree design approaches for mitigating daytime urban heat island effects in a high-density urban environment, *Energy Build.* 114 (2016) 265–274.
- [37] R.A. Spronken-Smith, T.R. Oke, The thermal regime of urban parks in two cities with different summer climates, *Int. J. Rem. Sens.* 19 (11) (1998) 2085–2104.
- [38] E. Ng, et al., A study on the cooling effects of greening in a high-density city: an experience from Hong Kong, *Build. Environ.* 47 (2012) 256–271.
- [39] Census, H.K.S.A.R. Statistics Department, Population and Household Statistics Analysed by District Council District, 2018, Edition, 2018.
- [40] P.K. Cheung, C.Y. Jim, Comparing the cooling effects of a tree and a concrete shelter using PET and UTCI, *Build. Environ.* 130 (2018) 49–61.
- [41] T.C. Lee, K.Y. Chan, GINN Projection of extreme Temperatures in Hong Kong in the 21st century, *Acta Meteorol. Sin.* 25 (1) (2010) 1–20.
- [42] L.H. Yeung, S.M. Song, Communicating Climate Change Messages in Hong Kong, 2016.
- [43] C. Ren, E.Y.-y. Ng, L. Katzschnier, Urban climatic map studies: a review, *Int. J. Climatol.* 31 (15) (2011) 2213–2233.
- [44] S. Tsoka, A. Tsikaloudaki, T. Theodosiou, Analyzing the ENVI-met microclimate model's performance and assessing cool materials and urban vegetation applications—A review, *Sustain. Cities Soc.* 43 (2018) 55–76.
- [45] Y. Yang, et al., The “plant evaluation model” for the assessment of the impact of vegetation on outdoor microclimate in the urban environment, *Build. Environ.* 159 (2019) 106151.
- [46] T. Mohammad, S. David, A.B.-W. George, Micrometeorological simulations to predict the impacts of heat mitigation strategies on pedestrian thermal comfort in a Los Angeles neighborhood, *Environ. Res. Lett.* 11 (2) (2016), 024003.
- [47] S. Thorsson, et al., Different methods for estimating the mean radiant temperature in an outdoor urban setting, *Int. J. Climatol.* 27 (14) (2007) 1983–1993.
- [48] W.F. Lamb, et al., Learning about urban climate solutions from case studies, *Nat. Clim. Change* 9 (4) (2019) 279–287.
- [49] I.D. Stewart, Redefining the Urban Heat Island, 2011.
- [50] R. Wang, et al., Mapping the local climate zones of urban areas by GIS-based and WUDAPT methods: a case study of Hong Kong, *Urban climate* 24 (2018) 567–576.
- [51] J.E. Nichol, et al., Urban heat island diagnosis using ASTER satellite images and ‘in situ’ air temperature, *Atmos. Res.* 94 (2) (2009) 276–284.
- [52] C.Y. Jim, The status and prospects of urban trees in Hong Kong, *Landsc. Urban Plann.* 14 (1987) 1–20.
- [53] K. Blaizejczyk, et al., Comparison of UTCI to selected thermal indices, *Int. J. Biometeorol.* 56 (3) (2012) 515–535.
- [54] S. Provençal, et al., Thermal comfort in Quebec City, Canada: sensitivity analysis of the UTCI and other popular thermal comfort indices in a mid-latitude continental city, *Int. J. Biometeorol.* 60 (4) (2016) 591–603.
- [55] H. Lee, H. Mayer, L. Chen, Contribution of trees and grasslands to the mitigation of human heat stress in a residential district of Freiburg, Southwest Germany, *Landsc. Urban Plann.* 148 (2016) 37–50.
- [56] L. Chen, et al., Sky view factor analysis of street canyons and its implications for daytime intra-urban air temperature differentials in high-rise, high-density urban areas of Hong Kong: a GIS-based simulation approach, *Int. J. Climatol.* 32 (1) (2012) 121–136.
- [57] A. Middel, et al., Impact of urban form and design on mid-afternoon microclimate in Phoenix Local Climate Zones, *Landsc. Urban Plann.* 122 (2014) 16–28.
- [58] E. Ng, Policies and technical guidelines for urban planning of high-density cities - air ventilation assessment (AVA) of Hong Kong, *Build. Environ.* 44 (7) (2009) 1478–1488.
- [59] T. Loridan, C.S.B. Grimmond, Characterization of energy flux partitioning in urban environments: links with surface seasonal properties, *Journal of Applied Meteorology and Climatology* 51 (2) (2011) 219–241.
- [60] H. Fan, et al., How to cool hot-humid (Asian) cities with urban trees? An optimal landscape size perspective, *Agric. For. Meteorol.* 265 (2019) 338–348.
- [61] B. Jiang, et al., A dose-response curve describing the relationship between tree cover density and landscape preference, *Landsc. Urban Plann.* 139 (2015) 16–25.
- [62] C.Y. Jim, A planning strategy to augment the diversity and biomass of roadside trees in urban Hong Kong, *Landsc. Urban Plann.* 44 (1) (1999) 13–32.
- [63] Department-HKEDD, H.K.C.E.a.D., Greening Master Plan (GMP), 2010.
- [64] Department-HKPD, H.K.P., Hong Kong Planning Standards and Guidelines, 2010.